Jurnal Kejuruteraan (*Journal of Engineering*) Submission http://dx.doi.org/10.17576/jkukm-2019-31(1)
10 pages
ISSN: 0128-0198 e-ISSN: 2289-7526
*Revision : 20190920*

# Experimental Investigation on the Parameters Influencing Local Scour Types around Scaled Triangular Nose Bridge Pier in Nonuniform Mobile Bed

## (Penyiasatan Eksperimen terhadap Parameter yang Mempengaruhi Jenis KerukanTempatan di sekitar Bucu Segi Tiga Tiang Sambut Berskala dalam Dasar Mudah Alih Tidak Seragam)

Huda Rasool A.[a], Thamer Ahmed Mohammed[a] & Nordila Ahmad[b*]

[a]*Department of Water Resources Engineering, College of Engineering, University of Baghdad, 10070 Jadireyah, Baghdad, Iraq,*
[b]*Faculty of Engineering, National Defence University of Malaysia, Sungai Besi Camp, 57000 Kuala Lumpur, Malaysia.*
**Corresponding author: (Email: nordila@upnm.edu.my)*
*Received 25th May 2024, Received in revised form 13th September 2024*
*Accepted 1st October 2024, Available online 30th November 2024*

ABSTRACT

*The local scour at the triangular nose pier of the Al Kufa bridge, Kufa, Iraq was experimentally investigated using a pier model with a scale of 1:155. Special arrangements were followed to fix the pier model in the middle of the mobile bed with nonuniform sediments of median diameter, $d_{50}$=0.30 mm and geometric standard deviation, $\sigma_g$=2.78. The mobile bed had a depth of 100 mm and a length of 2m and was located 6 m from the inlet of a glass-sided titling flume. For five different discharges, the effect of flow parameters (velocity, u, water depth, y and Froude number, Fr), pier dimensions (pier width, b and pier length, l), bed sediment characteristics ($d_{50}$, $\sigma_g$ and threshold velocity for sediments, $u_t$) and time, t on local scour depth were studied. Throughout the experiments, clear water scour and lived bed scour were achieved. For clear water conditions, the relationship between normalized scour depth ($d_s$/b) and velocity ratio was found almost linear up to $u_a/u_t$=1 while for live bed scour conditions, a nonlinear relationship with a decreasing trend was found. For the thin pier, the laboratory data obtained from the present study demonstrated that the depth of the local scour ($d_s$) was independent of the water depth. When Fr=0.061 in both model and prototype, the measured scour depth at the pier model was overestimated by 0.4 m at the pier of Al Kufa Bridge. In addition, a relationship between scour depth ratio ($d_s/d_{seq}$) and time ratio ($t/t_{seq}$) was prepared from laboratory data. The relationship is useful in determining the equilibrium scour depth at the Al Kufa Bridge. Furthermore, the angle of the scour holes ($\theta$) resulted from the equilibrium scour depth was measured and found to be ranges between 14° and 18.4°.*

*Keywords: Local scour, pier model, Al Kufa bridge, nonuniform sediments, governing parameters*

*ABSTRAK*

*Ketidakselesaan pemandu telah menjadi tumpuan terutamanya di kalangan pihak yang berkepentingan. Terdapat pelbagai faktor yang menyumbang kepada ketidakselesaan ketika memandu, yang melibatkan kedua-dua nya iaitu pemandu dan komponen dalaman kereta. Dalam kajian ini, penyelidikan ke atas pengecutan otot bagi bahagian bawah kaki pemandu ketika mengendalikan pedal pemecut telah dilakukan. Objektif utama kajian ini ialah bagi menentukan corak pengecutan otot apabila mengendalikan pedal pemecut dalam tiga aksi berbeza; tekan, separa tekan dan lepas. Untuk memeriksa corak pengecutan otot ini, sebelas peserta telah dipilih untuk terlibat dalam eksperimen pemanduan bersimulasi dalam makmal. Penderia elektromyografi permukaan (SEMG) telah digunakan untuk mengukur aktiviti otot untuk bawah kaki, yang dikenali sebagai Tibialis Anterior (TA). Pengukuran SEMG dilakukan dengan menempatkan elektrod pada permukaan kulit dan aktiviti elektrik pada kanan TA di bawahnya direkodkan. Data mentah daripada penderia SEMG telah ditapis menggunakan tiga frekunesi berbeza, laluan tinggi, takuk dan laluan rendah. Kemudiannya, nilai Punca Min Kuasa Dua (RMS) akan dihasilkan berdasarkan peratusan Pengecutan Maksima Sukarela (%MVIC). Prosedur pengumpulan data ke atas otot terpilih adalah berdasarkan cadangan Surface Electromyography for the Non-Invasive Assessment of Muscles (SENIAM). Hasil kajian ini menunjukkan bahawa TA mempamerkan pengecutan otot tertinggi ketika aksi melepaskan. Sebagai penutup, otot TA berkerja secara berbeza bergantung kepada aksi pedal kereta.*

*Kata Kunci: Kerukan tempatan, model tiang sambut, jambatan Al Kufa, sedimen tidak seragam, parameter yang mengawal*

Jurnal Kejuruteraan (*Journal of Engineering*) Submission http://dx.doi.org/10.17576/jkukm-2019-31(1)
10 pages
ISSN: 0128-0198 e-ISSN: 2289-7526
*Revision : 20190920*

## INTRODUCTION

Reports showed that most of the bridges around the world failed due to severe local scour at the bridges substructure. Razi, et al., (2011) conducted laboratory tests to study the impact of bed sills at cylindrical piers with clear water flow conditions on the reduction of local scour depth. Physical modelling had been implemented in the laboratory to determine how a skewed integrated bridge would scour under a flood condition (Akib, et al., 2012). Khassaf and Shakir (2013) modelled the local scour at Al Kufa Bridge using HEC-RAS. Based on laboratory tests, Khassaf et al. (2014) observed the level of local scour near bridge piers when a bed sill downstream was used as a preventative measure. They used a model of a pier with a circular section under water flow conditions. The local scour depth was decreased using bed sills placed at various distances from the pier downstream and with varying widths and thicknesses. Bridge pier scour model with non-uniform sediments studied by Pournazeri, et al. (2014). The goal of the study was to create a three-dimensional scour prediction model and validate it with measurements made in a lab.
Experimental investigation methodology was followed by Ismael, et al.( 2015) to study the impact of changing the bridge pier site with flow direction on the reduction in scour depth. Dahe and Kharode (2015) used HEC-RAS to determine the extent of scour at bridge piers with different geometric designs. Wang, et al. (2016) performed laboratory tests to research the regional scour near double cylindrical piers in an open channel. The research revealed that the scour hole at twin cylindrical piers was generated by clear water scour, and it was almost identical to that formed by the same scour type around a single cylindrical pier. Ahmad et al. (2017) proposed a new empirical relation for the estimation of the non-dimensional maximum scour depth for a wide pier as a function of the sediment coarseness. Statistical methods verified the proposed method, reducing the root mean square error from 71% to 26%. Yilmaz et al. (2017) proposed a semi-empirical model to estimate the temporal variation of clear water scour depth at identical cylindrical piers. The experiments included various pier sizes, pier spacings, and flow intensities. The probabilistic methodology proposed by Tubaldi et al. (2017) for the evaluation of clear water scour around bridge piers by comparing the equilibrium scour depth associated with peak-flow discharges of return periods between 100 to 200 years with the foundation depth of the bridge. Moussa (2018) estimated the local scour at piers with different geometries by using one dimensional and two-dimensional mathematical models. The Aswan and El Minia bridges were selected since these bridges were considered major bridges in Egypt. Omara and Tawfik (2018) proposed a numerical model for local scour prediction around bridge piers considering how the pier cross section affects the model prediction. The findings of the computations have been validated using various published experimental data. The ptimal bridge pier layout for scour reduction was studied by employing a single pier with a square collar, a circular collar, and the interaction of two piers in a laboratory channel. The goal of the laboratory experiments was to determine the best size and placement of a single pier's collar in relation to the interaction of two piers (Al-Shukur and Ali, 2019). In order to restore the Barboni and Al-Qadisiyah Bridges in the Al-Muthanna Governorate, Iraq, GIS techniques such as dynamic color coding and visualization techniques were used by Wattan and Al-Bakri (2019). Khassaf and Ahmed (2020) experimentally studied the effect of external factors such as pier shapes and flow intensity on local scour depth around rectangular, oblong, and hexagonal pier shapes and they found that the best shape is a hexagonal pier, which gives the minimum local scour depth. Jalal and Hassan (2020) studied the impact of bridge pier shape on scour depth by using a methodology that was based on computational fluid dynamics (CFD) and the Flow-3D model. Scour at a bridge on the Kabul River, Pakistan was studied by Noor et al. (2020) using physical and HEC-RAS Modelling. They conducted analysis of both circular and square piers for comparison purposes, despite the real pier shape being round. Al-Hassani and Mohammad (2021) conducted a series of experiments on a laboratory flume to ascertain the effect of the silt location of a wire on the size of the scour area and depth formed at upstream. Local scour at complex bridge piers in Bangladesh rivers was studied by Mondal (2022). On a national scale, the study evaluated local scour at 239 bridges in Bangladesh. The hydrologic, hydraulic, and sediment data needed for the assessment were obtained from primary measurements, samples, numerical models and secondary sources. Bridge piers scour under the combined action of waves and current was studied by Kumar and Afzal (2023) using physical modelling. Predictions obtained from the application of various available formulae used to estimate the scour depth under combined wave–current flow in the coastal environment were compared with experimental measurements. Baranwal and Das (2024) presented a comprehensive analysis of scour depths obtained from predictive equations for clear-water and live-bed scouring conditions. The study intends to compile existing empirical equations suitable for calculating equilibrium scour depth around a bridge pier under clear water and live bed scour conditions, as well as available experimental

Jurnal Kejuruteraan (*Journal of Engineering*) Submission http://dx.doi.org/10.17576/jkukm-2019-31(1)
10 pages
ISSN: 0128-0198 e-ISSN: 2289-7526
*Revision : 20190920*

and field data sets on various types of bridge pier scouring and the impact of flow and roughness parameters on both clear water scouring and live bed scouring.
The reviewed literature revealed that the majority of the published studies were focused on the estimation

of scour depth at the location piers in the mobile bed. However, this study focused on studying the variables influencing scour types at the site of a triangular nose pier model located in a nonuniform mobile bed. Also, the impact of low flows and high flows or river hydrographs on the scour depth was studied. Basically, most of the riverbed materials are of a nonuniform nature. The pier geometry and bed sediments used in the laboratory experiments were identical to those of Al Kufa Bridge.

## MATERIALS AND METHODS

### Case study and field measurement

Al Kufa Bridge is a main bridge in Al Najaf City, Iraq and it was constructed in 1954. Figure 1 shows a general view of the bridge. A large number of vehicles are crossing the bridge daily and the safety of the bridge is very important to the public. There is no continuous monitoring of the bridge to ensure its safety. Scour at the bridge is one of the causes that affect bridge safety. There is no data on the scour at Al Kufa Bridge. In the present study, field measurements on the scour at Al Kufa Bridge were conducted. In addition, a laboratory model was used to estimate the depth of scour under various flow circumstances. Modelling can help to reduce the cost of design and maintenance for a bridge. Figure 1 shows a general view for the studied bridge .

FIGURE 1. A general view of Al Kufa bridge

### Cross Sections Survey at Al Kufa Bridge Using M9 Device

M9 device was used to survey 7 sections in the vicinity of Al Kufa Bridge. The locations of the sections were carefully decided to cover sections upstream, at the pier location and downstream. More details on the surveyed sections are shown below:

- Section A-A is 50 metres from the bridge in the upstream (Figure 2)
- Section B-B is 6 metres from the nose of the piers upstream (Figure 2)
- Section C-C is 1 meter from the pier's nose upstream (Figure 2)
- Section D-D at the point of the triangular nose of the piers upstream (Figure 2)
- Section E-E in the middle of the piers of the bridge (Figure 2)
- Section F-F at the point of the triangular nose of the piers downstream (Figure 2)
- Section G-G at 5 metres from the pier nose downstream (Figure 2)
-

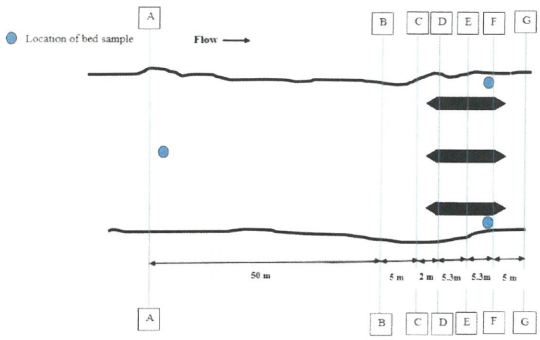


Note: the drawing is not to scale

FIGURE 2. Plan for Al Kufa Bridge showing the locations of the bridge piers, cross-sections and sampling points

FIGURE 3. Measurement of bed levels, water depths and velocities using the M9 device

The bed level coordinates in x, y and z obtained from M9 device are shown in Figure 3. The SURFER programme was used to plot the topography of the river at the Al Kufa Bridge site as shown in Figure 4. At each point in the river section, data obtained from M9 device included water depths, velocity and discharge. Figure 5 shows a cross section of the Euphrates River obtained from the M9 device at the Al Kufa bridge site.

Jurnal Kejuruteraan (*Journal of Engineering*) Submission http://dx.doi.org/10.17576/jkukm-2019-31(1)
10 pages
ISSN: 0128-0198 e-ISSN: 2289-7526
*Revision : 20190920*

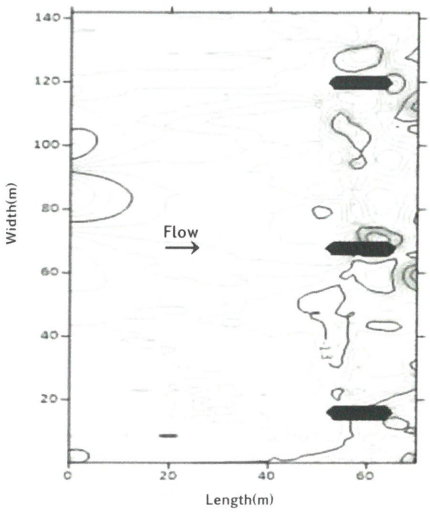


FIGURE 4. The bed topography of the Euphrates River at Al Kufa Bridge

Experimental work

The tests were carried out on a glass-sided tilting flume with a bed width of 0.3m, a total length of 12m and a total depth of 0.3m. The pier of Al Kufa Bridge was scaled down and the pier model was fixed tightly n a working section of 2m long. Non-uniform sedment with a median diameter ($d_{50}$) of 0.3mm was used to fill the working section up to a depth of 10cm. The pier model (made of steel and painted to prevent corrosion) was fixed tightly in the working section. The width of the working section was 0.3m (the same width as the flume) and located 5 m from the flume inlet. At the flume inlet, a special arrangement was used to control the effect of turbulence on the mobile bed. was used to control the effect of turbulence on the mobile bed. Furthermore, two identical ramps with a gentle slope of 1(vertical):10 (horizontal) were employed right upstream and downstream of the working section.
The function of the upstream ramp was to create a smooth flow transition from the flume bed to the mobile bed of the working section, while the function of the downstream ramp was to maintain a smooth n flow transition from the section of work to the original flume bed. Figure 6 shows a profile for the working section including the upstream and downstream ramps. Figure 7 shows the grading curve for the nonuniform sediments used in this study. The bed sediment used in the working section was $d_{50}$=0.3 mm and the calculated geometric standard deviation, $\sigma_g$ was found to be 1.7.The following formula was used for the determination of the geometric standard deviation of the sediments.

$$\sigma_g = \sqrt{\frac{d_{84}}{d_{16}}} = \sqrt{\frac{0.5}{1.7}} = 1.7 > 1.3 \quad (1)$$

where $d_{84}$ and $d_{16}$ sediment sizes were obtained from the grading curve shown in Figure 7.

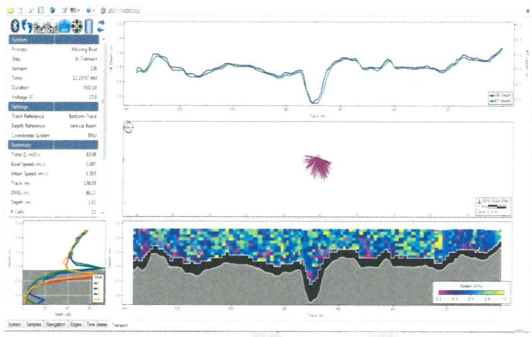

FIGURE 5. A sample of the data obtained from the M9 device.

The function of the upstream ramp was to create a smooth flow transition from the flume bed to the mobile bed of the working section, while the function of the downstream ramp was to maintain a smooth n flow transition from the section of work to the original flume bed. Figure 6 shows a profile for the working section including the upstream and downstream ramps.

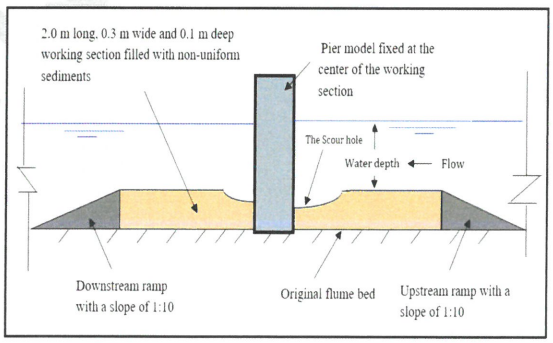


FIGURE 6. The flume exhibits a longitudinal profile at the location of working section

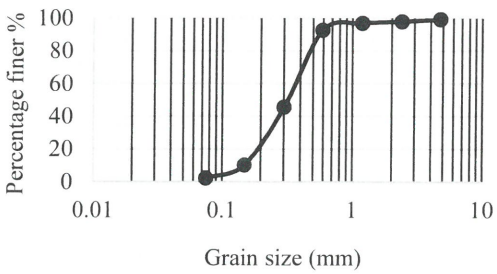


FIGURE 7. The grading curve for the bed sediments in the working section

Jurnal Kejuruteraan (*Journal of Engineering*) Submission http://dx.doi.org/10.17576/jkukm-2019-31(1)
10 pages
ISSN: 0128-0198 e-ISSN: 2289-7526
*Revision : 20190920*

Figure 8 shows the actual pier dimensions and the dimensions of the pier model. The model of the Al Kufa bridge pier was made of steel with a scale of 1:155. The scale was decided based on the space available inside the flume compared with that at Al Kufa Bridge.

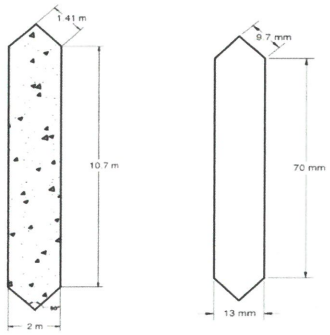


a. Al Kufa bridge pier b. The pier model

FIGURE 8. Section in the piers of prototype and model

Five experiments with different discharges were conducted and after the completion of each experiment, the depths of scour at every 0.5 mm around the hole of scour were estimated by using a point gauge with acceptable accuracy Figure 9.

FIGURE 9. The point gauge

After measuring the approach velocity and water depth in the flume, the flows were categorized based on the value of the Froude number as steady and subcritical (values of the calculated Froude number were less than 1). The depth of water was measured by the point gauge. The maximum scour depths were measured at 15 min, 30 min, 60 min, 120 min, 240 min, 480 min, 720 min, 960 min, 1200 min, and 1440 min from the commencement of each experiment.

Factors Influence Local Scour at Pier Bridge

The factors affecting local scour depth at a bridge constructed in a straight stream with alluvial sediments are flood flow, bed sediment, bridge geometry and time. This can be presented in the following equation:

$$d_s = \begin{bmatrix} (river\ discharge), (bed\ material), \\ (bridge\ geometry), (time) \end{bmatrix} \quad (2)$$

Since the bridge geometry for Al Kufa Bridge is not a variable, it is discarded from Eq. (2) and only the pier width (b) will be considered.
The flowing water is affected by water density (ρ), kinematic viscosity (ν), acceleration due to gravity (g), approach velocity ($u_a$), water depth (y), and the lateral distribution of the flow in the approach channel (G) resulting from the shape of the approach channel cross section.
In addition, the characteristics of bed sediment are governed by the median size of the sediment ($d_{50}$), geometric standard deviation ($\sigma_g$), sediment density ($\rho_s$) and threshold velocity of the sediment ($u_t$).
The time (t) is an important factor that affects the local scour depth at bridges and (ϕ) is a function. Eq. (2) can be written as

$$d_s = f\emptyset[(\rho, \nu, u_a, y, g, G), (d_{50}, \rho, \rho_s, u_t), (t)] \quad (3)$$

In this study, a single type of sediment which represents the mobile bed in the Euphrates River at the site of Al Kufa Bridge was used which means that $\rho_s$, $\sigma_g$, and $d_{50}$ have known values and can be discarded from the studied variable. In addition, the effect of water density can also be discarded since a negligible change in temperature during the experiments is expected. The effect of the lateral distribution of the flow in the channel (G) is neglected since the tested pier model will be conducted in a straight laboratory flume with a fixed rectangular cross section. Eq. (3) became

$$d_s = \phi[(u_a, y, g), (u_t), (b), (t)] \quad (4)$$

After conducting the dimensional analysis using the π theorem, the above equation can be written in dimensionless form as

$$\frac{d_s}{b} = \phi\left[\frac{u_a}{u_t}, \frac{y}{b}, \frac{u_a}{\sqrt{g\,b}}, \frac{u_a\,t}{b}\right] \quad (5)$$

where, $\frac{u_a}{u_t}$ is the velocity ratio, $\frac{y}{b}$ is the normalized flow depth, $\frac{u_a}{\sqrt{g\,b}}$ is the pier Froude number and $\frac{u_a\,t}{b}$ is the dimensionless time ratio for scour development.

Jurnal Kejuruteraan (*Journal of Engineering*) Submission http://dx.doi.org/10.17576/jkukm-2019-31(1)
10 pages
ISSN: 0128-0198 e-ISSN: 2289-7526
*Revision : 20190920*

## RESULTS AND DISCUSSION

### Uniformity of sediment and scour type

The grading curve was plotted after conducting sieve analysis on the bed materials taken from three different locations in the Euphrates River at the site of the Al Kufa Bridge. The geometric standard of deviation of Euphrates River bed material ($\sigma_g$) confirmed the nonuiformity of the river bed material. In addition, the median size of the river bed material ($d_{50}$) was found to be 0.30 mm. However, nonuniform sediments with $d_{50}$=0.3 mm waere used in the working section. This showed that a material with the same characteristics was used in the model. In this study, a constant value for the sediment size ratio (model pier width (b) relative to the sediment size ($d_{50}$)) was used for all test runs ($b/d_{50}$ =43). The triangular nose piers for Al Kufa Bridge have a length of 12.7 m and a width of 2 m, while the triangular nose pier model has a length of 84.5 mm and a width of 13 mm. This showed that the scale used was 1:155.
To determine if the flow is transporting bed material from the approach channel just upstream of the pier site (i.e., live-bed scour), the threshold velocity that can remove the median size ($d_{50}$) or smaller sizes from the channel mobile bed ($u_t$) should be compared with the mean approach velocity ($u_a$). If $u_t>u_a$, then the scour type is clear water otherwise it is a live bed. For determining the critical velocity of the sediments in the mobile bed, the equation proposed by Laursen (1963) can be used for this purpose. In this study, five runs were implemented and the scour type corresponding to each run was checked. Table 1 shows the flow conditions with the resulting scour type.

For runs number 1 and 2, the scour type was clear water since the values of $u_a/u_t< 1$. However, the scour type was live bed for runs number 3, 4 and 5 since the vales of $u_a/u_t>1$ Table 1. Bridges constructed in natural streams or rivers may have live bed scour at higher discharges of the hydrograph and clear water scour at lower discharges of the hydrograph. It is important to cover both scour types in the test runs of the present study since the prototype (the Al Kufa Bridge) was constructed in the Euphrates River and high and low discharges may pass in the river

TABLE 1. The characteristics of the test runs

| Run No. | Discharge (l/s) | Water Depth, y (cm) | Approach Velocity($u_a$) (cm/s) | Critical Velocity($u_t$) (cm/s) | $u_a/u_t$ | Pier Width in lab.(mm) | Scour Type |
|---|---|---|---|---|---|---|---|
| 1 | 2.100 | 17.5 | 4.0 | 31 | 0.13 | 13 | Clear Water |
| 2 | 3.384 | 4.70 | 24 | 25 | 0.96 | 13 | Clear Water |
| 3 | 4.050 | 5.00 | 27 | 25 | 1.08 | 13 | Live Bed |
| 4 | 4.770 | 5.30 | 30 | 25.5 | 1.17 | 13 | Live Bed |
| 5 | 7.360 | 6.80 | 36 | 27 | 1.33 | 13 | Live Bed |

The scour is a process depending on time. Therefore, scour depths were measured after 15 min, 30 min, 45 min, 60 min, 120 min, 240 min, 480 min, 960 min, and 1440 min from the commencement of each test run. Figures 10 to 14 show the measured scour depth with the time for 5 test runs. The variation of scour depths with time was different in clear water scour than in live bed scour. In live bed conditions, the migration of bed form causes fluctuation of the scour depth with time, and this is related to the balance between the scouring caused by the flowing water and the sediments resistance to motion which is progressively attained through erosion. At equilibrium, for sand and gravel beds, the local scour depth ($d_{seq}$) is developing more rapidly in the live bed compared with that developing under the clear water scour. Hence, it is recommended to consider peak scour depth for live bed conditions as a critical value in the bridge design since the peak local scour depth associated with clear water conditions may not be attained and require much longer time (Melville and Coleman, 2000).

### The Effects of Governing Dimensionless Parameters on Local Scour Depth

Eq. (4) shows the dimensionless parameters governing the local scour depth are velocity ratio ($u_a/u_t$), normalized flow depth (y/b), sediment size ratio ($b/d_{50}$), pier Froude number ($Fr_b$) and dimensionless time ratio for scour development ($u_at/b$). The laboratory data was used to plot the relation between the normalized scour depth ($d_s/b$) and velocity ratio ($u_a/u_t$) for nonuniform sediment used in the mobile bed of the working section Figure 15. The behavior of the clear water scour depth was almost linear up to $u_a/u_t$=1 and after that the local scour became live bed and nonlinear with a decreasing trend. For live bed scour type, the correlation of the normalized scour depth ($d_s/b$) and flow depth ratio (y/b) is shown in Figure 16.

Jurnal Kejuruteraan (*Journal of Engineering*) Submission http://dx.doi.org/10.17576/jkukm-2019-31(1)
10 pages
ISSN: 0128-0198 e-ISSN: 2289-7526
*Revision : 20190920*

(Melville and Coleman, 2000) showed that for b/y< 0.7, the local scour depth will increase directly with the pier width (b) and it is independent of the water depth (y). In other words, this happens when the pier is narrow (the flow depth is greater than the pier width). In the present study and for $b/d_{50}$=43, the relationship between normalized depth of scour and normalized depth of flow was found to be in agreement with that presented by (Melville and Coleman, 2000) for $b/d_{50}$=50.

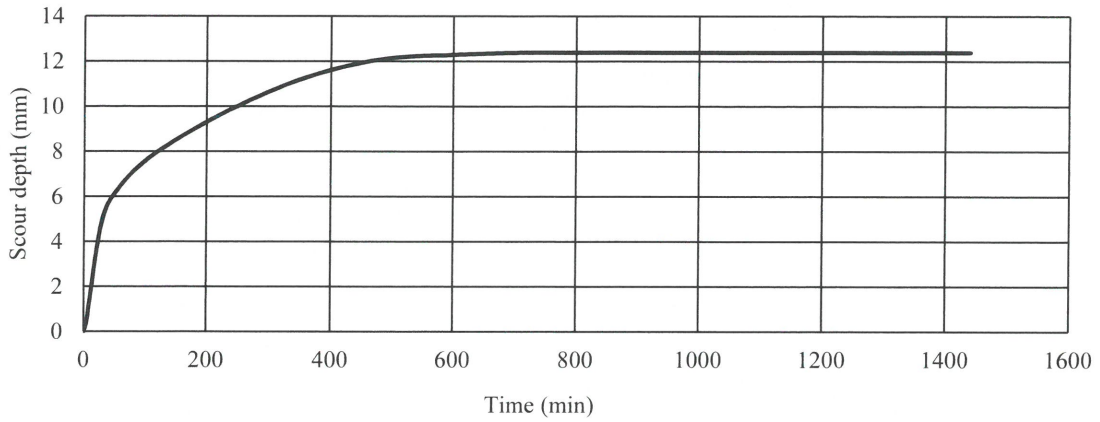


FIGURE 10. Variation of the depth of scour with time for the first run (Q= 2.10 l/s)

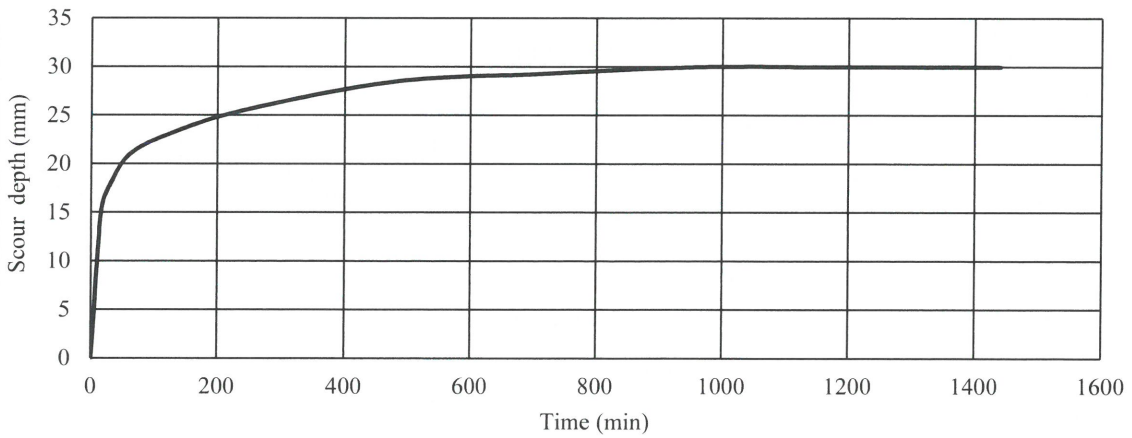


FIGURE 11. Variance in depth of scour with time for the second run (Q= 3.384 l/s)

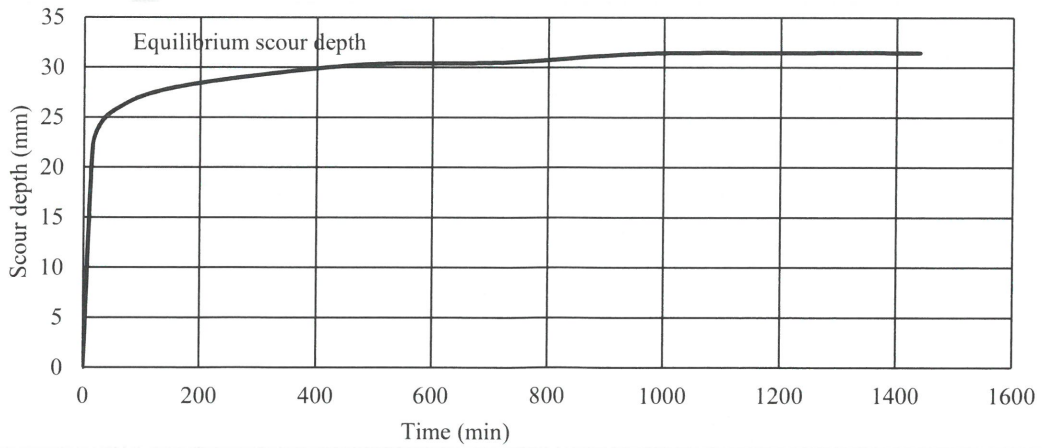


FIGURE 12. Variance in depth of scour with time for the third run (Q= 4.050 l/s)

Jurnal Kejuruteraan (*Journal of Engineering*) Submission http://dx.doi.org/10.17576/jkukm-2019-31(1)
10 pages
ISSN: 0128-0198 e-ISSN: 2289-7526
*Revision : 20190920*

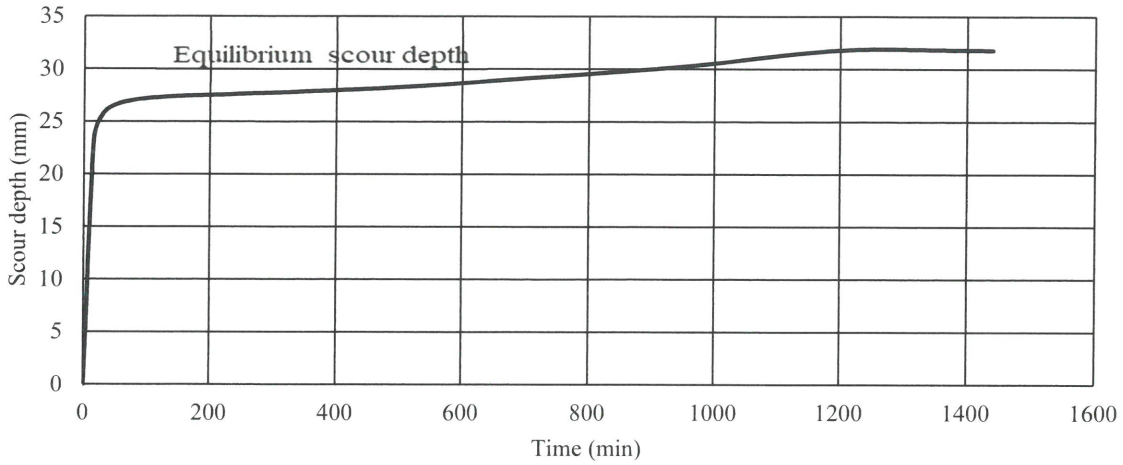


FIGURE 13. Variance in depth of scour with time for the fourth run (Q= 4.770 l/s)

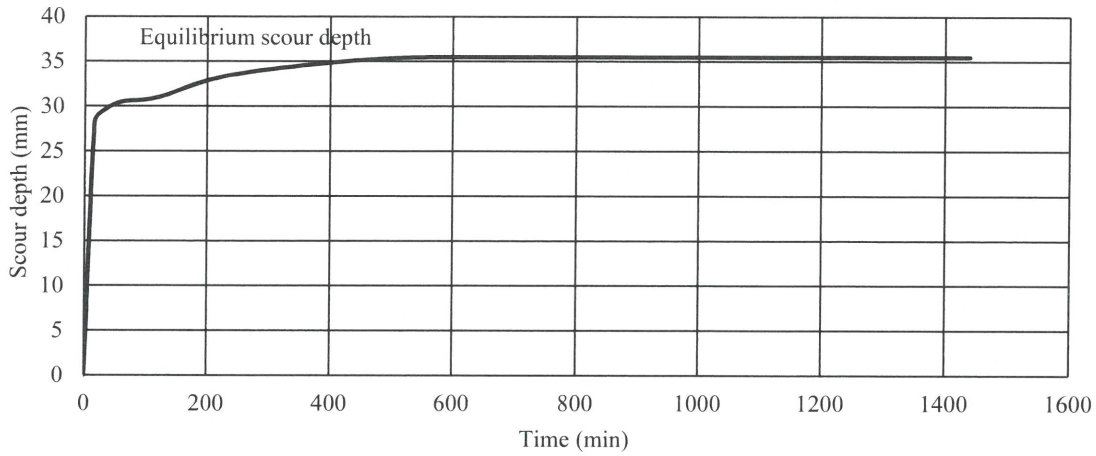


FIGURE 14. Variance in depth of scour with time for the fifth run (Q= 7.360 l/s)

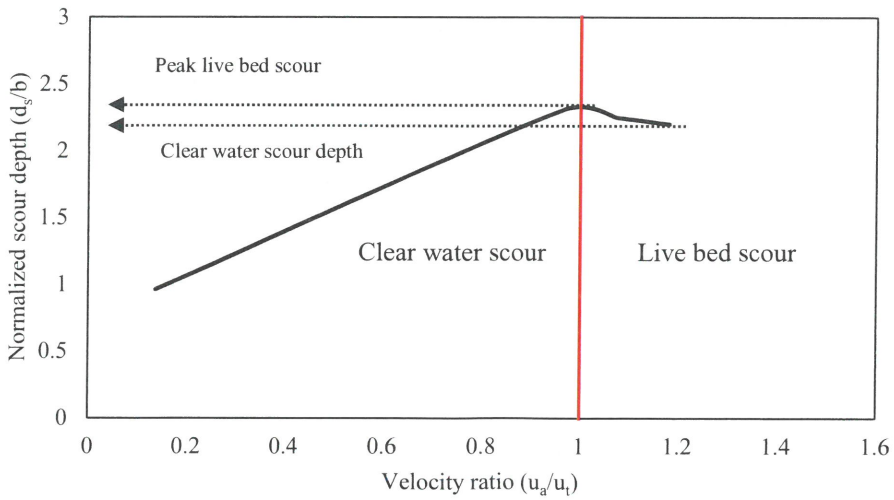


FIGURE 15. Variance of normalized depth of scour ($d_s/b$) with the velocity ratio ($u_a/u_t$)

Jurnal Kejuruteraan (*Journal of Engineering*) Submission http://dx.doi.org/10.17576/jkukm-2019-31(1)
10 pages
ISSN: 0128-0198 e-ISSN: 2289-7526
*Revision : 20190920*

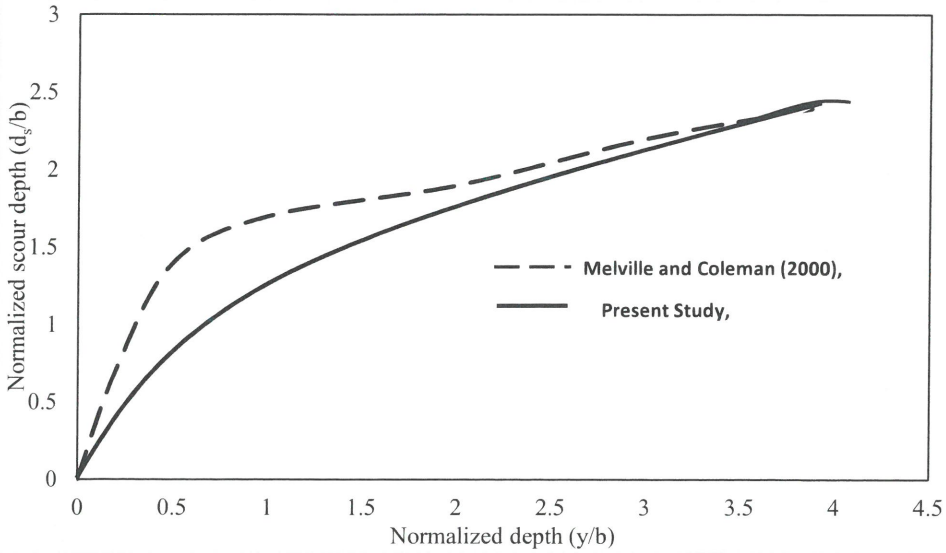


FIGURE 16. Variance of normalized scour depth ($d_s$/b) with normalized depth (y/b)

Another parameter affecting the local scour is the Froude number. According to Eq. (4), the Pier Froude number influences the depth of the scour. The laboratory data of the present study was used to demonstrate the effect of the pier Froude number on local scour depth Figure 17. Melville and Coleman (2000) suggested to include the effect of pier Froude number in the estimation of local scour at bridges at the design stage (before construction). However, in the present study it is suggested to use the data on the pier model to estimate the local scour depth at Al Kufa Bridge. The kinematic similarity stipulates that the Froude number in both the laboratory flume and in the Euphrates River near Al Kufa Bridge should be equal. The approach velocity and water depth in the Euphrates River near Al Kufa bridge were measured using the M9 device and they were found to be 0.33m/s and 2.9m respectively. The field data was used to calculate the Froude number in the prototype near the location of Al Kufa Bridge and it was found to be 0.061. In addition, plots were made showing the normalized scour depth's relationship to the Froude number as shown in Figure 18. The scour depth for flow conditions expected to occur in the Euphrates River near the Al Kufa bridge can be estimated using Figure 18. For example, when the value of Fr= 0.061, the scour depth was found to be 2.1 m. However, the measured scour depth by using the M9 device at the location of the middle pier of Al Kufa Bridge was found to be 1.7 m. This study revealed an absolute error of 0.4 m between the model and the prototype. According to Ettema, et al. (1998), results on local scour obtained from model studies conducted in the laboratory were greater than the scour depth that was likely to occur in the prototype. This justifies the difference of 23% between the values of scour depths in both the model and prototype.

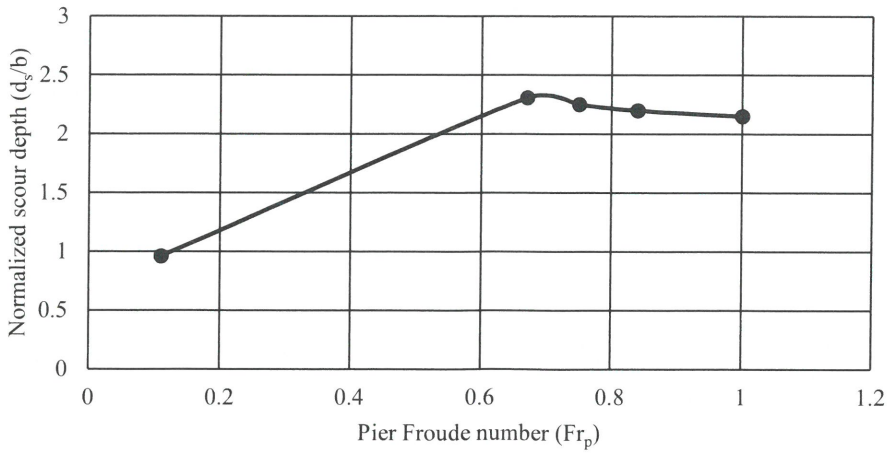


FIGURE 17. Variance of scour depth with pier Froude number

Jurnal Kejuruteraan (*Journal of Engineering*) Submission http://dx.doi.org/10.17576/jkukm-2019-31(1)
10 pages
ISSN: 0128-0198 e-ISSN: 2289-7526
*Revision : 20190920*

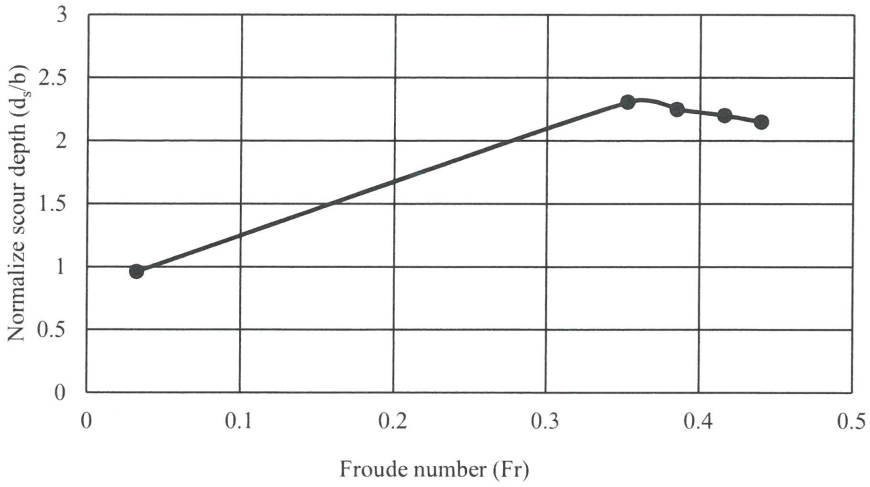


FIGURE 18. The variance of depth of scour and the Froude number

The time required to get the equilibrium depth of scour ($t_{seq}$) was found to be dependent on lower values of the normalized flow depth (y/b) and independent of y/b for higher values or when the piers are thin. Thus, the variables affecting $t_{seq}$ were given by Melville and Chiew (1999) in a dimensionless form as

$$\frac{u_a t_{seq}}{b} = f\left(\frac{u_a}{u_t}, \frac{y}{b}, \frac{b}{d_{50}}\right) \quad (6)$$

$$t^* = \frac{u_a t_{seq}}{b} \quad (7)$$

where t* is the dimensionless time ratio for equilibrium scour depth

In this study, the pier width and sediments used in the working section were not changed; therefore, the value of $b/d_{50}$ became constant and discarded from the dimensionless parameters affecting $t_e$. Eq. (5) became as,

$$t^* = f\left(\frac{u_a}{u_t}, \frac{y}{b}\right) \quad (8)$$

For a constant value of $b/d_{50}$, the experimental data on the local scour time confirmed the dependence of t* on $u_a/u_t$ and y/b only. The t* increases with y/b for low flow depths and is independent of y/b for high flow depths. Figure 19 shows that the influence of normalized flow depth on t* occurs up to a value of y/b that is approximately equal to 4 where the maximum value of t* was found to be approximately equal to 1.65 x $10^6$. For clear water scour depths, the value of t* increased rapidly with $u_a/u_t$ until it reached maximum at the value of $u_a/u_t$= 1. For live bed scour conditions and when the values of $u_a/u_t$ became more than one, t* rapidly decreased as shown in the dashed line in Figure 20. Live bed scour conditions are typically occurring during floods and flood duration will estimate if the equilibrium live bed scour depth will develop or not.

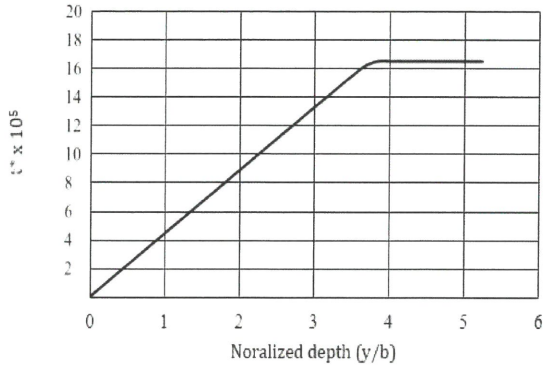


FIGURE 19. Variation of t* with normalized depth

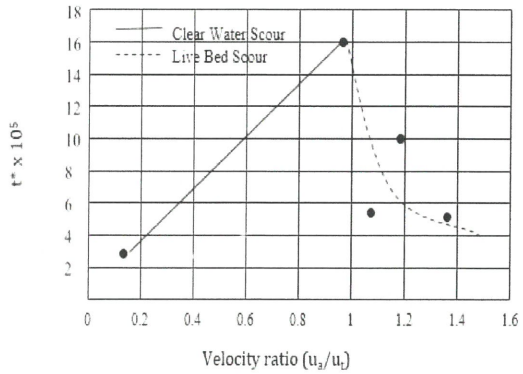


FIGURE 20. Variation of t* with velocity ratio ($u_a/u_t$)

Jurnal Kejuruteraan (*Journal of Engineering*) Submission http://dx.doi.org/10.17576/jkukm-2019-31(1)
10 pages
ISSN: 0128-0198 e-ISSN: 2289-7526
*Revision : 20190920*

When the maximum flood passes, the river hydrograph shows a recession of flow and clear water scour conditions may prevail for the duration of the falling limb of the hydrograph. Therefore, the period of the flow recession could increase the scour depth, particularly when near threshold velocity is maintained over a considerable period (Melville and Coleman, 2000). However, Melville and Chiew (1999) showed that both $t_{seq}$ and $d_{seq}$ are affected by flow and sediment properties since they are inherently interdependent. This justifies why $t_{seq}$ for the live bed scour type was less than that for the clear water scour type. In this study, data on $d_s/d_{seq}$ with $t/t_{seq}$ was plotted on a logarithmic scale for various runs or various velocity ratios ($u_a/u_t$) as shown in Figure 21. The resulting plots in Figure 21 were different and it mainly depending on $u_a/u_t$ and scour type. Higher values of $u_a/u_t$ (live bed scour) resulted in a flatter curvature, while lower values of $u_a/u_t$ (clear water scour) resulted in a steeper curvature. Compared with the equilibrium scour depth under live bed conditions, the scour depth for clear water conditions developed asymptotically towards the equilibrium depth in longer time. For test runs with a live bed, the equilibrium depth of scour developed rapidly and fluctuated afterward. The scour depth's variations are attributed to the continuous movement of sediments (Melville and Coleman, 2000).

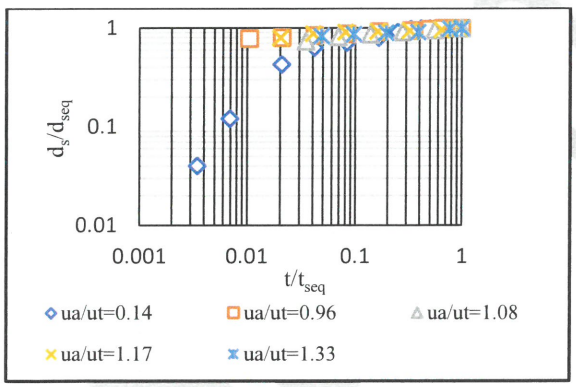


FIGURE 21. Variance of scour depth ratio ($d_s/d_{seq}$) with time ratio ($t/t_{seq}$) for various velocity ratio

The scour depth's variations are attributed to the continuous movement of sediments (Melville and Coleman, 2000). The scour hole formed around the pier model was measured. The scour depths were measured after dividing the scour hole into grids and each one was 5mm x 5mm, but grids in important locations were 2mm x 2mm in dimensions. In order to determine the scouring volume and to demonstrate the counters of the scour hole around the pier model, data on scour depths after each run were measured manually using a point gauge with an accuracy of ±1mm and fed to the Surfer® program. Figure 22 shows the two dimensional representations of the hole of scour. However, Figure 23 shows the variance of the volume of scour with the discharge.

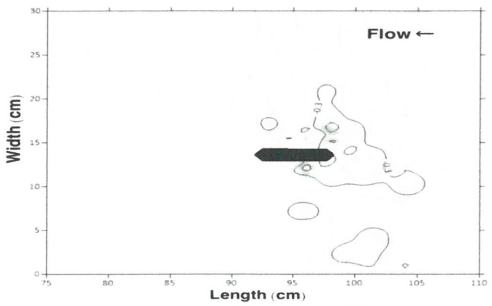


a. Contours of the hole of scour for the first run (Q= 2.10 l/s)

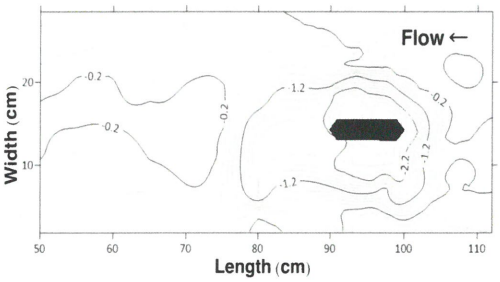


b. Contours of the hole of scour for the second run (Q= 3.384 l/s)

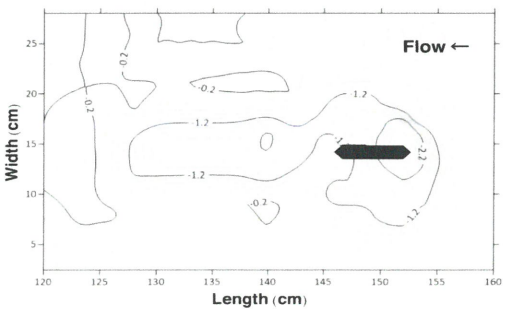


c. Contours of the hole of scour for the third run (Q= 4.050 l/s)

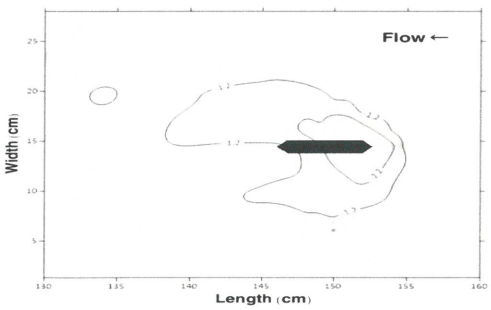


d. Contours of the hole of scour for the fourth run (Q= 4.770 l/s)

Jurnal Kejuruteraan (*Journal of Engineering*) Submission http://dx.doi.org/10.17576/jkukm-2019-31(1)
10 pages
ISSN: 0128-0198 e-ISSN: 2289-7526
*Revision : 20190920*

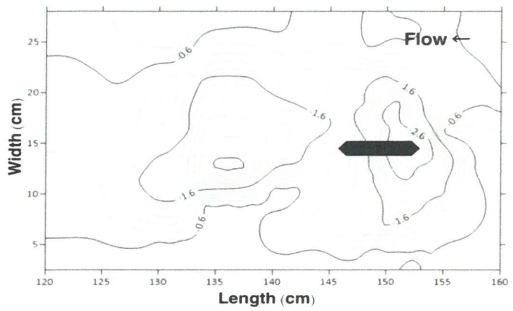


e. Contours of the hole scour for the fourth run (Q= 7.360 l/s)

FIGURE 22. Contours for the scour around the pier model for different runs

Angle and Size of the Scour Hole

The scour hole formed around the pier model was measured. The scour depths were measured after dividing the scour hole into grids and each one was 5mm x 5mm, but grids in important locations were 2mm x 2mm in dimensions. In order to determine the scouring volume and to demonstrate the counters of the scour hole around the pier model, data on scour depths after each run were measured manually using a point gauge with an accuracy of ±1mm and fed to the Surfer® program. Figure 22 shows the two dimensional representations of the hole of scour. However, Figure 23 shows the variance of the volume of scour with the discharge.

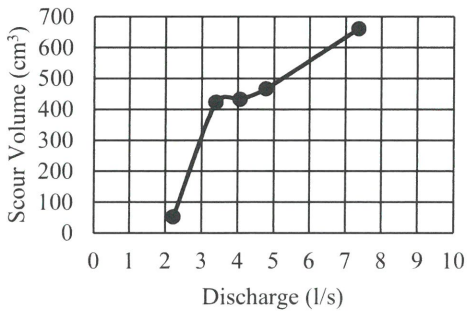


FIGURE 23. Variation of scour volume with flume discharge

From the laboratory data, the profile of the hole of scour was plotted using a relevant scale. The angle of the scour hole (θ) for each run was determined. It was found that the angles of the scour holes in Figures 24a and 24b were identical and equal to 14° while those in Figures 25c and 24d were found to be 17.5° and 18.4° respectively.

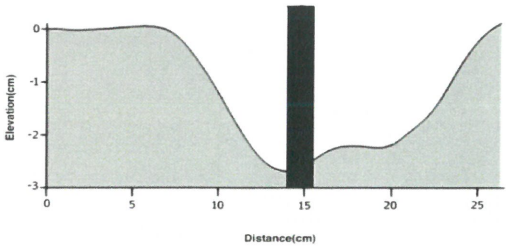


a. Profile of the hole of scour for second run

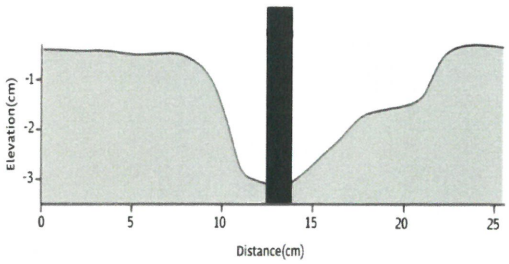


b. Profile of the hole of scour for third run

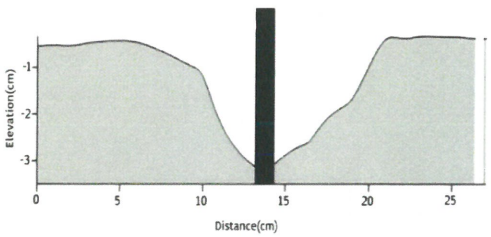


c. Profile of the hole of scour for fourth run

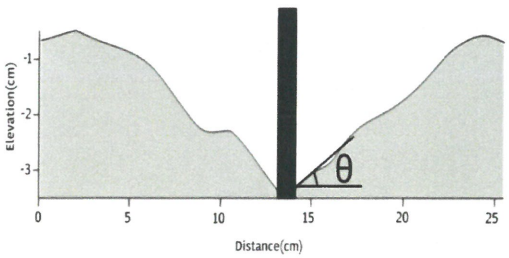


d. Profile of the hole of scour for fifth run

FIGURE 24. Profiles of the scour holes

CONCLUSION

In this research, the scour depths at Al Kufa Bridge were measured using M9 device. For describing the bed material at the bridge site, three samples were taken from the vicinity of the bridge and the grading curve showed that the bed material at the bridge site was nonuniform with a geometric standard deviation

Jurnal Kejuruteraan (*Journal of Engineering*) Submission http://dx.doi.org/10.17576/jkukm-2019-31(1)
10 pages
ISSN: 0128-0198 e-ISSN: 2289-7526
*Revision : 20190920*

($\sigma_g$) of 1.7 and a median particle size ($d_{50}$) of 0.30 mm. A scale of 1:155 was used to model the triangular nose pier of the Al Kufa bridge. In the laboratory, nonuniform sediments with $d_{50}$= 0.30 mm were used to fill the 2 m working section up to 100 mm. The working section was located in a laboratory flume with 12m in length, 0.30m in width and 0.30m in depth. The pier model was fixed in the mobile bed and tested using five runs of different discharges that were covered with clear water and live bed scour types. For each run, the temporal variation of scour depth was monitored. According to the dimensional analysis, the dimensionless parameters governing the local scour were velocity ratio ($u_a/u_t$), normalized water depth ($d_s/b$), pier Froude number ($Fr_p$) and time. For a real representation of the flow in the Euphrates River at the Al Kufa Bridge, the laboratory experiments covered both the clear water and live bed scours. During higher flows, Al Kufa bridge bridges was subjected to live bed scour, while it was subjected to clear water scour during lower flows. In the laboratory experiments, runs number 1 and 2 covered the clear water scour ($u_a/u_t<1$) while runs number 3, 4 and 5 covered the live bed scour ($u_a/u_t>1$). For fine-grained material (sands), results of the present study confirmed that the equilibrium local scour depth ($d_{seq}$) was rapidly developed in live bed conditions, while it took a longer time to develop in clear water scour conditions. For all test runs, the values of b/y range from 0.075 to 0.28 which is less than 0.7 and falls under the category of narrow piers, where the depth of scour is mainly dependent on pier width only. For equilibrium scour depth, the variation of the dimensionless time ratio (t*) with flow intensity was almost linear for the clear water scour ($t_{seq}$ was increased directly with the increase in $u_a$) and it was nonlinear for the live bed scour ($t_{seq}$ was decreased with the increase in $u_a$). The dimensionless time ratio for equilibrium scour depth was increased with y/b for low flow depths and became independent of y/b for high flow depths. From the model results, the Froude number was utilized to establish a scour depth formula for Al Kufa Bridge. A difference of 0.4 m between the model and the prototype was found and this confirmed that results from model studies in the laboratory always gave greater scour depth compared with that measured in the field. The logarithmic relationship between $d_s/d_{seq}$ and $t/t_{seq}$ can be utilized to establish the scour depth at Al Kufa Bridge. For the pier model, the angle of the scour hole ($\theta$) was found to range between 14° and 18.4°.

ACKNOWLEDGEMENT

The authors highly acknoledge the technical support from the Department of Water Rescources Engineering, College of Engineering, University of Baghdad and the financial support from the the [b]Faculty of Engineering, National Defense University.

REFERENCES

Ahmad, N., Mohammad, T. A., & Suif, Z. 2017. Prediction of local scour around wide bridge piers under clear-water conditions. *GEOMATE Journal 12*(34): 135-139.

Ahmed, S. I., & Khassaf, S. I. 2020. Study the local scour around different shapes of non-uniform piers. *Basrah J Engg Sci 20*(1): 12-14.

Akib, S., Jahangirzadeh, A., Wei, L. H., Shirazi, S. M., & Rahman, S. 2012, August. Experimental study on the skewed integral bridge by using crushed concrete geobags as scour protection. In *Proceedings of the 6th International Conference on Scour and Erosion*: 197-203.

Al-Hassani, N. Z., & Mohammad, T. A. 2021. Impact of the Weir Slit Location, the Flow Intensity and the Bed Sand on the Scouring Area and Depth at the Dam Upstream. *Journal of Engineering 27*(5): 49-62.

Al-Shukur, A. H. K., & Ali, M. H. 2019. Optimum design for controlling the scouring on bridge piers. *Civ. Eng. J 5*(9): 1904-1916.

Baranwal, A., & Das, B. S. 2024. Scouring around bridge pier: a comprehensive analysis of scour depth predictive equations for clear-water and live-bed scouring conditions. *AQUA—Water Infrastructure, Ecosystems and Society*, jws2024235.

Dahe, P. D., & Kharode, S. B. 2015. Evaluation of scour depth around bridge piers with various geometrical shapes. *Evaluation 2*(7): 41-48.

Ettema, R., Mostafa, E. A., Melville, B. W., & Yassin, A. A. 1998. Local scour at skewed piers. *Journal of Hydraulic Engineering 124*(7): 756-759.

Ismael, A., Gunal, M., & Hussein, H. 2015. Effect of bridge pier position on scour reduction according to flow direction. *Arabian Journal for Science and Engineering 40*: 1579-1590.

Jalal, H. K., & Hassan, W. H. 2020. Effect of bridge pier shape on depth of scour. In *IOP conference series: materials science and engineering* (Vol. 671, No. 1, p. 012001). IOP Publishing.

Khassaf, S. I., & Shakir, S. S. 2013. Evaluation of the local scour around group piers (Babil bridge as case study). *International Journal*

*of Innovative Research in Science, Engineering and Technology 2*(12): 7409-7420.

Khassaf, S. I., Yost, S. A., & Abulwahed, A. A. 2013. Control of local scour depth around btidge pier using down strem bed sill. *Kufa Journal of Engineering 5*(1): 85-104.

Kumar, L., & Afzal, M. S. 2023. A review of the state of research on bridge pier scour under combined action of waves and current. *Acta Geophysica 71*(5): 2359-2379.

Laursen, E. M. 1963. An analysis of relief bridge scour. *Journal of the Hydraulics Division 89*(3): 93-118.

Melville, B. W., & Chiew, Y. M. 1999. Time scale for local scour at bridge piers. *Journal of Hydraulic Engineering 125*(1): 59-65.

Melville, B. W., & Coleman, S. E. 2000. *Bridge scour*. Water Resources Publication.

Mondal, M. S. 2022. Local Scour at Complex Bridge Piers in Bangladesh Rivers: Reflections from a Large Study. *Water 14*(15): 2405.

Moussa, A. M. A. 2018. Evaluation of local scour around bridge piers for various geometrical shapes using mathematical models. *Ain Shams Engineering Journal 9*(4): 2571-2580.

Noor, M., Arshad, H., Khan, M., Khan, M. A., Aslam, M. S., & Ahmad, A. 2020. Experimental and HEC-RAS modelling of bridge pier scouring. *Journal of Advanced Research in Fluid Mechanics and Thermal Sciences 74*(1): 119-132.

Omara, H., & Tawfik, A. 2018, May. Numerical study of local scour around bridge piers. In *IOP conference series: earth and environmental science* (Vol. 151, No. 1, p. 012013). IOP Publishing.

Pournazeri, S., Li, S. S., & Haghighat, F. 2014, October. A bridge pier scour model with non-uniform sediments. In *Proceedings of the Institution of Civil Engineers-Water Management* (Vol. 167, No. 9: 499-511. Thomas Telford Ltd.

Razi, S., Salmasi, F., Hosseinzadeh Dalir, A., & Farsadizaeh, D. 2011. Application of bed sill to control scouring around cylindrical bridge piers. *Journal of Civil Engineering and Urbanism 2*(3): 115-121.

Tubaldi, E., Macorini, L., Izzuddin, B. A., Manes, C., & Laio, F. 2017. A framework for probabilistic assessment of clear-water scour around bridge piers. *Structural safety 69*: 11-22.

Wang, H., Tang, H., Liu, Q., & Wang, Y. 2016. Local scouring around twin bridge piers in open-channel flows. *Journal of Hydraulic Engineering 142*(9): 06016008.

Wattan, S. A. A., & Al-Bakri, M. 2019. Development of Bridges Maintenance Management System based on Geographic Information System Techniques (Case study: AlMuthanna\Iraq). *Journal of Engineering 25*(7): 21-36.

Yilmaz, M., Yanmaz, A. M., & Koken, M. 2017. Clear-water scour evolution at dual bridge piers. *Canadian Journal of Civil Engineering 44*(4): 298-307.